Journal of Magnetic Resonance 244 (2014) 90–97

Contents lists available at ScienceDirect

Journal of Magnetic Resonance

journal homepage: www.elsevier.com/locate/jmr

Acceleration of natural-abundance solid-state MAS NMR measurements on bone by paramagnetic relaxation from gadolinium-DTPA

Kamal H. Mroue [a,b], Rongchun Zhang [a,b,d], Peizhi Zhu [b], Erin McNerny [c], David H. Kohn [c], Michael D. Morris [b], Ayyalusamy Ramamoorthy [a,b,*]

[a] Biophysics, The University of Michigan, Ann Arbor, MI 48109-1055, United States
[b] Department of Chemistry, The University of Michigan, Ann Arbor, MI 48109-1055, United States
[c] School of Dentistry, The University of Michigan, Ann Arbor, MI 48109-1055, United States
[d] School of Physics, Nankai University, Tianjin 300071, PR China

ARTICLE INFO

Article history:
Received 18 January 2014
Revised 27 March 2014
Available online 10 May 2014

Keywords:
Solid-state NMR
Paramagnetic relaxation enhancement
Ultrafast MAS
Gd-DTPA
Bone

ABSTRACT

Reducing the data collection time without affecting the signal intensity and spectral resolution is one of the major challenges for the widespread application of multidimensional nuclear magnetic resonance (NMR) spectroscopy, especially in experiments conducted on complex heterogeneous biological systems such as bone. In most of these experiments, the NMR data collection time is ultimately governed by the proton spin–lattice relaxation times (T_1). For over two decades, gadolinium(III)-DTPA (Gd-DTPA, DTPA = Diethylene triamine pentaacetic acid) has been one of the most widely used contrast-enhancement agents in magnetic resonance imaging (MRI). In this study, we demonstrate that Gd-DTPA can also be effectively used to enhance the longitudinal relaxation rates of protons in solid-state NMR experiments conducted on bone without significant line-broadening and chemical-shift-perturbation side effects. Using bovine cortical bone samples incubated in different concentrations of Gd-DTPA complex, the ^{1}H T_1 values were calculated from data collected by ^{1}H spin-inversion recovery method detected in natural-abundance ^{13}C cross-polarization magic angle spinning (CPMAS) NMR experiments. Our results reveal that the ^{1}H T_1 values can be successfully reduced by a factor of 3.5 using as low as 10 mM Gd-DTPA without reducing the spectral resolution and thus enabling faster data acquisition of the ^{13}C CPMAS spectra. These results obtained from ^{13}C-detected CPMAS experiments were further confirmed using ^{1}H-detected ultrafast MAS experiments on Gd-DTPA doped bone samples. This approach considerably improves the signal-to-noise ratio per unit time of NMR experiments applied to bone samples by reducing the experimental time required to acquire the same number of scans.

1. Introduction

Over the past decade or so, solid-state NMR (ssNMR) spectroscopy has advanced substantially to become the primary probe for the molecular structure and dynamics of a wide variety of systems, ranging from small inorganic and organic materials to large biological macromolecules like crystalline peptides and proteins, amyloid fibrils and membrane-bound systems [1–5]. In addition, numerous recent studies have demonstrated that ssNMR using magic angle spinning (MAS) is particularly well-suited for mapping the structural and dynamic features of heterogeneous non-crystalline biomaterials that are difficult to characterize by solution NMR spectroscopy and diffraction methods, such as bone and related connective tissues [6–17]. It is well known that bone represents one of nature's most challenging and exciting biological materials [18–20]. This is due to the complex hierarchical structural organization of bone which, at the macroscopic level, is composed of a rigid inorganic mineral (mainly poorly crystalline carbonated hydroxyapatite) and a soft organic matrix (largely type I collagen, along with ~10% of various non-collagenous proteins, lipids, polysaccharides, and citrates) that mutually interact and contribute to bone biomechanical properties and functions [8,10,20–22]. Water is the third major component of bone, and is found at multiple locations: it occupies the Ca^{2+} coordination sites within the mineral crystal lattice; it is bound to collagen fibrils; and a significant portion exists as free bulk water that fills the microscopic pores in the calcified matrix [16,17,23]. Thus, understanding the molecular interactions among the different constituents and the specific role of each is of prime significance in order to gain high-resolution

* Corresponding author at: Biophysics and Department of Chemistry, The University of Michigan, Ann Arbor, MI 48109-1055, United States. Fax: +1 (734) 764 3323.
E-mail address: ramamoor@umich.edu (A. Ramamoorthy).

http://dx.doi.org/10.1016/j.jmr.2014.04.020
1090-7807/

insights into the structure–function relationship in bone. In this regard, one- and two-dimensional ^{1}H, ^{13}C, and ^{31}P MAS ssNMR have been the most widely used methods for the atomic-level structural elucidation of bones [6–17].

In spite of the wealth and diversity of information that it can provide about molecular structure and dynamics, one of the major challenges for the widespread application of ssNMR spectroscopy on macromolecular complex systems is its intrinsic poor sensitivity that originates mainly from the very small spin population difference between magnetically induced nuclear spin states in thermal equilibrium [24,25]. This issue of low sensitivity is particularly evident in the context of ssNMR spectroscopy of bone due to its complex heterogeneous and low-crystalline structure, which is reflected as low resolution of the obtained NMR line shapes relative to the chemical shift range. Thus, several hours or even days of signal averaging are required to obtain an acceptable signal-to-noise ratio (S/N) in multidimensional experiments that involve detection of dilute nuclei like ^{13}C through cross-polarization from the more abundant protons. In these measurements, the total NMR experimental time is determined largely by the inter-scan recycle delay, which in turn depends on the ^{1}H spin–lattice (or longitudinal) relaxation time (T_1) and is necessarily set long enough (typically ~5 times ^{1}H T_1) in order to fully relax the proton magnetization to thermal equilibrium and also to minimize the duty cycle of the NMR probe and to avoid probe arcing and sample overheating due to continuous radiofrequency (*rf*) irradiation [26–28]. Generally, several approaches can be implemented in order to improve the signal intensity in NMR experiments [29,30]: increasing the sample quantity, isotopic enrichment, using ultra-high field NMR spectrometers, lowering the temperature, or utilizing the cutting-edge dynamic nuclear polarization (DNP)-based experiments.

One alternative simple approach for enhancing the signal, known as paramagnetic relaxation enhancement (PRE), is to introduce a small amount of a paramagnetic reagent into the targeted macromolecular lattice that will enable faster recovery of the ^{1}H equilibrium magnetization, which allows the use of shorter recycle delays and subsequently faster repetition rates, which result in a higher S/N per unit time [31]. Transition metals (e.g., Cu^{2+}, Ni^{2+}, Mn^{2+}), inner-transition metals (e.g., lanthanides) and the stable nitroxide free radicals that cause considerable PRE have proven to be particularly useful for fulfilling this desired effect [32].

In light of the above, signal enhancement through the longitudinal PRE effects of various paramagnetic dopants have been successfully explored in solution [26,33–37] and in solid-state NMR studies [27,38–48] on microcrystalline peptides, proteins, and membrane-bound systems. For instance, Ishii and co-workers have developed the "paramagnetic relaxation-assisted condensed data collection" (PACC) method [27,40], which relies on a combination of copper(II)-EDTA (Cu-EDTA) doping, very fast MAS (~40 kHz), and fast recycling of the low-power *rf* pulses to significantly accelerate multidimensional NMR experiments on hydrated microcrystalline proteins. Reif and co-workers have demonstrated that the combined use of Cu-EDTA doping and perdeuteration of proteins can induce further signal enhancement in MAS ssNMR experiments without significant loss of resolution [42,43]. Our group and others have shown that a very low concentration of copper-chelated lipid is sufficient enough to substantially reduce the proton T_1 values for faster data acquisition in a lipid bilayer or isotropic bicelles containing a membrane protein with minimum effect on spectral resolution [38,39,44]. In a very recent study, Glaubitz and co-workers have shown that gadolinium paramagnetic complexes can be used to significantly reduce the measurement time in MAS ssNMR experiments conducted on a 7TM membrane protein in lipid bilayers [48].

While the previous ssNMR studies have successfully explored the use of paramagnetic dopants to enhance the longitudinal relaxation in MAS NMR measurements of crystalline macromolecules, the PRE effects induced by these reagents on complex heterogeneous biomolecules like bone have not been investigated in depth. In a recent work [49], we have demonstrated that by immersing bovine cortical bone samples into a 30 mM Cu-EDTA solution, it was feasible to reduce the ^{1}H T_1 values by a factor of 2.2, thus allowing for faster acquisition of natural-abundance ^{13}C CPMAS (cross-polarization magic angle spinning) [50] spectra without significant line-broadening side effects nor chemical shift perturbations. Here, we extend our efforts toward investigating the possibility of further shortening the ^{1}H T_1 values in natural-abundance ^{13}C CPMAS ssNMR spectra of bone via the incorporation of more suitable paramagnetic metal ions, for the ultimate goal of increasing the sensitivity of these NMR spectra. In this context, chelated complexes of the gadolinium ion (Gd^{3+}) are well suited to address the desired goal, owing to the presence of seven unpaired electrons in the inner 4*f* orbitals of Gd^{3+} and its large magnetic moment [51,52]. By virtue of its isotropic magnetic susceptibility tensor, Gd^{3+} possesses unique paramagnetic properties in that while it causes larger PRE than other lanthanides, it does not cause any perturbations in the NMR chemical shifts [32]. These favorable paramagnetic properties, along with its relatively long electronic spin relaxation times (in the range of nano to microseconds) due to its symmetric S-state, make Gd^{3+} an attractive choice as a relaxation enhancement agent in carbon-detected MAS ssNMR experiments with magnetization starting on protons. For these reasons, gadolinium-based chelates have been widely used as contrast-enhancement agents in medical magnetic resonance imaging (MRI), as a tool for clinical diagnosis of organ and tissue abnormalities [51]. Among these complexes, [Gadolinium(III)-DTPA]$^{2-}$ (henceforth referred to as Gd-DTPA, DTPA = Diethylene triamine pentaacetic acid) stands out as the first contrast agent to be approved for clinical use in 1988 [51]. In this work, we have conducted a comprehensive concentration-dependent study to demonstrate that Gd-DTPA (Fig. 1) can also be effectively used to enhance the longitudinal relaxation rates of protons in natural-abundance ^{13}C CPMAS ssNMR experiments on bone tissues without significant line-broadening side effects and chemical shift perturbations in the ^{13}C NMR line shapes. Using bovine cortical bone samples incubated in solutions with different concentrations of Gd-DTPA complex, the ^{1}H T_1 values were calculated from a series of data collected by ^{1}H spin-inversion recovery method detected in ^{13}C CPMAS NMR experiments. Our results reveal that the ^{1}H T_1 time constants can be successfully reduced by a factor of 3.5 using as low as 10 mM Gd-DTPA without any loss of spectral resolution and thus enabling faster data acquisition of the ^{13}C CPMAS spectra at natural abundance. We further investigated the combined effect of very fast MAS and Gd-DTPA doping on the sensitivity in proton-detected solid-state NMR experiments applied to the bone

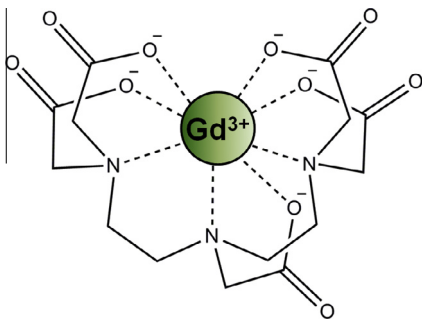

Fig. 1. Chemical structure of the Gd-DTPA complex used as a paramagnetic dopant in this study to shorten the spin–lattice relaxation times of protons from bone samples.

samples. Despite the reduced sample quantity used in the ultrafast MAS experiments, we observed about 3-fold gain in overall S/N per unit time of the ^{1}H MAS NMR spectra in the presence of 10 mM Gd-DTPA at 50 kHz MAS, which illustrates the ability for much faster data acquisition on extremely limited sample quantities.

2. Experimental details

2.1. Sample preparation

Powdered bovine cortical bone samples, collected from fresh bovine femora, were prepared and stored according to our previously published procedure [49]. Gd-DTPA solutions with different concentrations were prepared by dissolving the required amount of powder gadopentetic acid (Diethylene triamine pentaacetic acid gadolinium(III) dihydrogen salt, Sigma Aldrich, St. Louis, MO, USA) in standard PBS buffer. Bone samples were soaked with Gd-DTPA solutions for about 30 min, and filtered for each NMR experiment.

Prior to proceeding with the NMR experiments for this study, it was crucial to confirm that the treatment of bone samples with Gd-DTPA complex would not produce undesired effects on the structure and stability of the mineral crystal lattice in bone due to the possible substitution of Gd^{3+} for Ca^{2+} ions within the mineral crystal lattice and/or in the hydrated surface layer of bone. Theoretically, the formation constants (logK) for the Ca-DTPA and Gd-DTPA complexes are 9.8 and 22.2, respectively [53]; the gadolinium complex is thus favored by over 12 orders of magnitude compared to the calcium complex. Conditional formation constants (pH dependent) of the two DTPA complexes are also expected to differ by the same order, and therefore the probability of exchanging gadolinium for calcium in the Gd-DTPA complex is practically null. This argument was confirmed experimentally by measuring the Ca^{2+} concentration in our bone samples without and with Gd-DTPA using inductively coupled plasma-optical emission spectroscopy (ICP-OES). The results show that the Ca^{2+} concentration in bone does not practically change in the presence of 60 mM Gd-DTPA ($[Ca^{2+}]$ = 144 ± 39 μg/L with 60 mM Gd-DTPA, and 154 ± 58 μg/L without Gd-DTPA). The addition of the Gd-DTPA complex to bone therefore does not cause any substitution of Gd^{3+} for Ca^{2+}.

2.2. Solid-state NMR experiments

All ^{13}C-detected solid-state NMR experiments were conducted at 11.75 T on an Agilent VNMRJ 500 MHz NMR spectrometer operating at a resonance frequency of 125.6 MHz for ^{13}C and 499.44 MHz for ^{1}H, and using a 3.2-mm triple-resonance MAS probe. The ^{13}C MAS spectra were acquired under 10 kHz MAS conditions at 25 °C using linear ramped cross-polarization (CP) pulse sequence [54] with a ^{1}H excitation pulse length of 2.5 μs and a CP contact time of 2 ms. For each experiment, 10,000 scans were accumulated, with recycle delays ranging from 1 to 3.5 s that were optimized for each sample. To decouple protons during signal acquisition, a 65 kHz two-pulse phase-modulation (TPPM) scheme was applied [55]. The ^{13}C NMR chemical shifts were referenced with respect to tetramethylsilane (TMS) using adamantane as a secondary external standard. The ^{1}H T_1 values were calculated from a series of data collected by ^{13}C-detected ramped CPMAS inversion recovery experiments, in which a ^{1}H π-pulse followed by an inversion recovery delay were introduced prior to the CP sequence. Seven data points with increasing inversion recovery delays were recorded for each sample. The recycle delays were set to 4 s for samples containing Gd-DTPA and 6 s for those without Gd-DTPA, and 2000 scans were accumulated for each inversion recovery data point. The integral signal intensities were measured

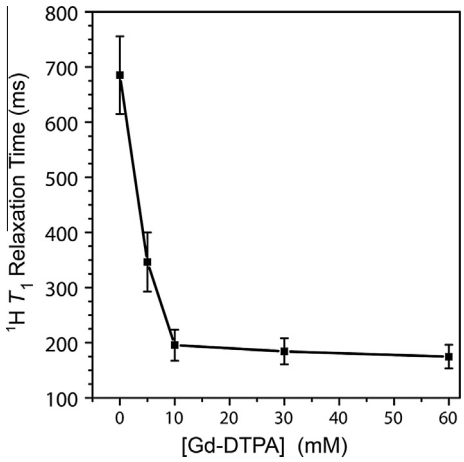

Fig. 2. Average ^{1}H spin–lattice relaxation time (T_1) of powdered cortical bone as a function of Gd-DTPA concentration. The ^{1}H T_1 values were determined from the ^{1}H spin-inversion–recovery method detected in ^{13}C ramped-CPMAS NMR experiments, and the reported errors were estimated from the best-fitting of experimental data.

for peaks in the aliphatic (10–70 ppm) and the carboxyl/carbonyl (165–185 ppm) regions to calculate the ^{1}H T_1 values for the individual amino acid residues. A mono-exponential function was used to calculate and analyze the ^{1}H T_1 values from the inversion recovery data using a script developed in the Ramamoorthy laboratory. The average of the ^{1}H T_1 values determined from all peaks was used as the ^{1}H T_1 value of the sample of interest.

All ^{1}H-detected MAS NMR experiments were acquired at 14.1 T (599.8 MHz ^{1}H resonance frequency) on an Agilent/Varian VNMRS 600 MHz solid-state NMR spectrometer, using a 1.2-mm triple-resonance ultrafast MAS probe at 25 and 50 kHz spinning speeds with a 1.2 μs 90° ^{1}H excitation pulse. The ^{1}H T_1 values for the bone samples were calculated from a series of data collected by ^{1}H-detected MAS inversion recovery experiments. The ^{1}H single-pulse and rotor-synchronized spin-echo (with a 0.6 ms inter-pulse delay) spectra were recorded with 64 scans each and an optimized recycle delay in the range of 1.2–5 s depending on the sample.

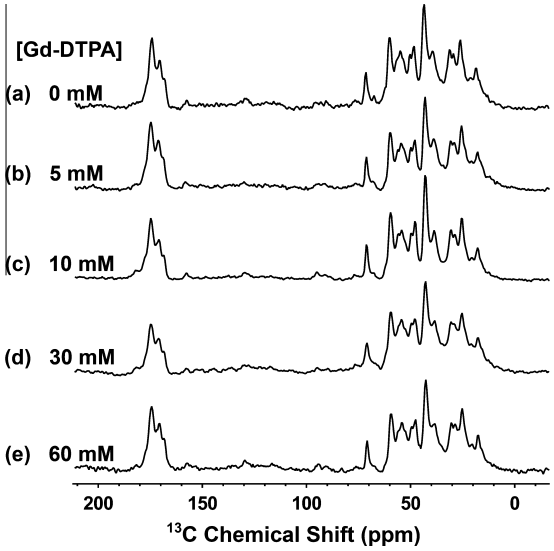

Fig. 3. Proton-decoupled ^{13}C CPMAS spectra recorded at 10 kHz MAS for (a) undoped bone, and (b–e) bone doped in different concentrations of Gd-DTPA (as indicated for each spectrum). All spectra were recorded under identical experimental conditions, except for the recycle delays that were set to ~5 × ^{1}H T_1 in an experimental time of: (a) 9.8 h, (b) 4.9 h and (c–e) 2.8 h.

3. Results and discussion

In this study, the concentration-dependent paramagnetic relaxation effects of Gd^{3+} ions on the proton intrinsic spin–lattice relaxation times measured in MAS NMR experiments on fresh bone samples are investigated for the purpose of accelerating the ssNMR data acquisition rate using the optimal dopant concentration. The ^1H T_1 relaxation times as a function of Gd-DTPA concentration were measured via ^1H spin inversion recovery method detected in ^1H to ^{13}C CPMAS NMR experiments (Supplementary Information). Fig. 2 shows the variation of the average ^1H T_1 for the bone samples as a function of the Gd-DTPA concentration. Overall, we observe that increasing the concentration of Gd-DTPA yields a gradually shorter T_1 time constants, and thereby faster relaxation rates. However, the T_1 relaxation times do not exhibit linear dependence on the Gd-DTPA concentration. A considerable reduction in ^1H T_1 is observed at lower Gd-DTPA concentrations (5 and 10 mM), while a much slower decrease in T_1 is achieved at higher Gd-DTPA concentrations. Accordingly, a 3.5-fold shortening in the ^1H T_1 time is observed with the addition of 10 mM Gd-DTPA. Further increase in the Gd-DTPA concentration to 30 mM and then to 60 mM results in only an additional minor decrease (<10%) in the ^1H T_1 time, which implies that the longitudinal PRE becomes almost saturated once this range of high concentrations is reached. This can be explained by realizing that ^1H PREs are mediated by a flexible ^1H–^1H spin-diffusion mechanism: the unpaired electrons of Gd^{3+} ions interact strongly with the close ^1H nuclei in the sample, which will significantly speed up the longitudinal relaxation of these nearby protons. This effect is further transferred to remote protons in the organic matrix via a ^1H-^1H spin-diffusion mechanism; this efficient diffusion process, by virtue of the high gyromagnetic ratio of protons, results in a uniform enhancement of the longitudinal relaxation rates for all protons in the sample [56]. At higher Gd-DTPA concentrations, it is most likely that this spin-diffusion process does not transfer the longitudinal PREs efficiently and uniformly throughout the organic–mineral interface in bones. It is therefore expected that since Gd-DTPA is hydrophilic, the ^1H magnetization is recovered more slowly at higher Gd-DTPA concentrations by paramagnetic longitudinal relaxation around the water-accessible organic–mineral interface.

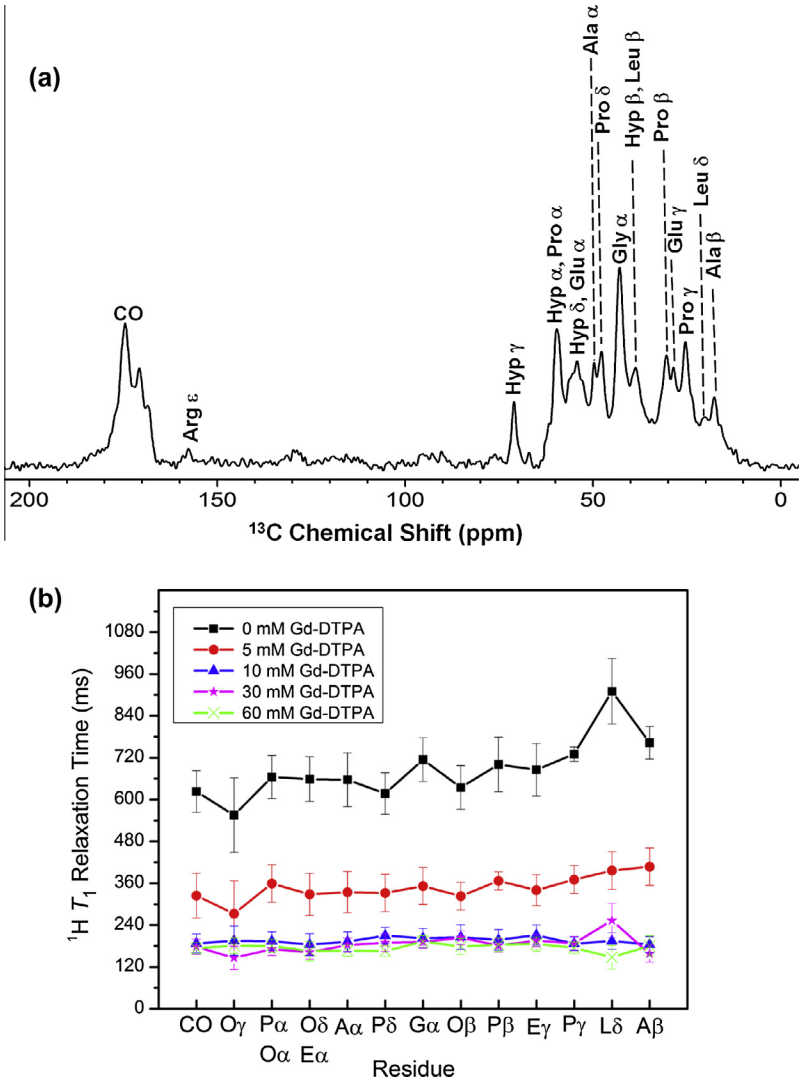

Fig. 4. (a) The ^{13}C NMR chemical shift assignments of various amino acids in the ^{13}C CPMAS spectrum of fresh cortical bovine bone. Ala, alanine; Leu, leucine; Pro, proline; Glu, glutamic acid; Hyp, hydroxyproline; Gly, glycine; Arg, arginine; CO, carbonyl. (b) Spin–lattice ^1H relaxation times (^1H T_1) of the various residues in powdered cortical bone doped in different concentrations of Gd-DTPA. The T_1 values were determined from ^1H-spin-inversion recovery detected in ^{13}C CPMAS NMR experiments, and the reported errors were estimated from the best-fitting of experimental data. A, alanine; L, leucine; P, proline; E, glutamic acid; O, hydroxyproline; G, glycine; CO, carbonyl. The signals from (Pα, Oα) and (Oδ, Eα) overlap in the ^{13}C NMR spectrum.

Meanwhile, it is instructive to compare the present results with those obtained in our previous study on the longitudinal PRE effect of Cu-EDTA on bone samples [49], in which a 2.2-fold enhancement in the ^{1}H relaxation rates was observed when bovine cortical bone samples were doped with 30 mM Cu-EDTA. Gd-DTPA is obviously a more efficient relaxation enhancement dopant than Cu-EDTA for bone. The better performance of Gd-DTPA might be explained in terms of the differences/similarities in the magnetic and structural properties exhibited by the two paramagnetic ions and their complexes. Gd^{3+} ion has seven unpaired electrons whereas Cu^{2+} possesses only one, with the unpaired electron spins of both ions relaxing relatively slowly (on the nanosecond time scale). Moreover, the magnetic susceptibility tensor of Gd^{3+} is totally isotropic, whereas that of Cu^{2+} is not totally isotropic [32]. Gd-DTPA is a nine-coordinate complex in which eight binding sites of the inner coordination sphere around the Gd center are occupied by the $(DTPA)^{5-}$ ligand while the ninth coordination site is occupied by a nearby water molecule [51]. Cu-EDTA, on the other hand, is a six-coordinate complex in which the $(EDTA)^{4-}$ ligand occupies all six binding sites at the Cu center, so that water is excluded as a first-coordination sphere ligand [52]. The presence of one water molecule directly coordinated to Gd, and the lack of it around Cu, might be one of the factors that contribute to the more efficient longitudinal PRE of Gd-DTPA over Cu-EDTA. It is quite plausible that the ^{1}H–^{1}H spin diffusion process is facilitated in the case of Gd-DTPA through the directly bonded water molecules at the bone mineral surface, and subsequently transferred to the water-bound collagen via the free bulk water within the bone pores. A second contributing factor is the larger size (mass) of Gd-DTPA molecules compared to Cu-EDTA. The larger molecular size of the Gd^{3+} complex reduces its mobility, which leads to enhanced relaxation rates through the increase of the rotational correlation time, which is one of the parameters that affect PRE rates.

Shown in Fig. 3 are the natural-abundance ^{13}C CPMAS NMR spectra for the doped bone samples in comparison with the undoped bone. These spectra were all collected under identical experimental conditions, except for the recycle delay, which was set to $\sim 5 \times$ ^{1}H-T_1 average value calculated from the spin inversion recovery experiments for each sample. It is evident that the recycle delay can be reduced considerably without loss of spectral resolution, resulting in a better S/N per unit time by shortening the data collection time required to acquire the same number of scans. In the presence of 5 mM Gd-DTPA, a 2-fold faster data acquisition is obtained, whereas a 3.5-fold faster acquisition is obtained upon the addition of 10 mM Gd-DTPA and more, which can achieve a twofold improvement in the S/N per unit instrumental time. Not surprisingly, the NMR line shapes in all these spectra are dominated by carbon resonances of the amino-acid residues in type I collagen, the major organic component in bones. Most of these resonances can be effortlessly identified, and hence assigned based on previously reported values [12,15,57], as shown in Fig. 4a for the ^{13}C CPMAS spectrum of untreated fresh bone. It is apparent from Fig. 3 that no major perturbations in the ^{13}C NMR chemical shifts are caused upon addition of various amounts of Gd-DTPA. It is well known that in addition to PRE, paramagnetic ions can cause the so-called pseudo-contact shifts (PCSs), which are reflected as changes in NMR chemical shift values of the nuclear spins that sense the paramagnetic center. PCSs originate mainly from through-space

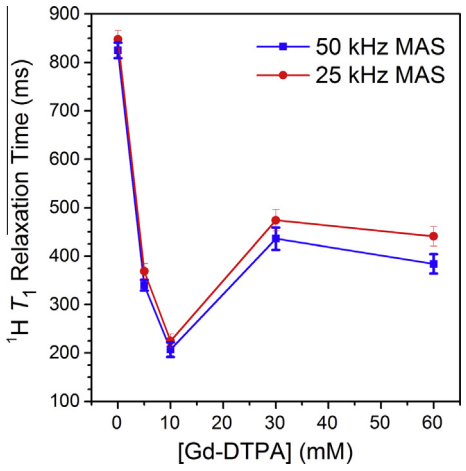

Fig. 6. Average ^{1}H spin–lattice relaxation time (T_1) of powdered cortical bone as a function of Gd-DTPA concentration. The ^{1}H T_1 values were determined by ^{1}H spin-inversion–recovery methods in ^{1}H-detected NMR experiments with 25 (red) and 50 (blue) kHz MAS rates. The reported errors were estimated from the best-fitting of experimental data. (For interpretation of the references to colour in this figure legend, the reader is referred to the web version of this article.)

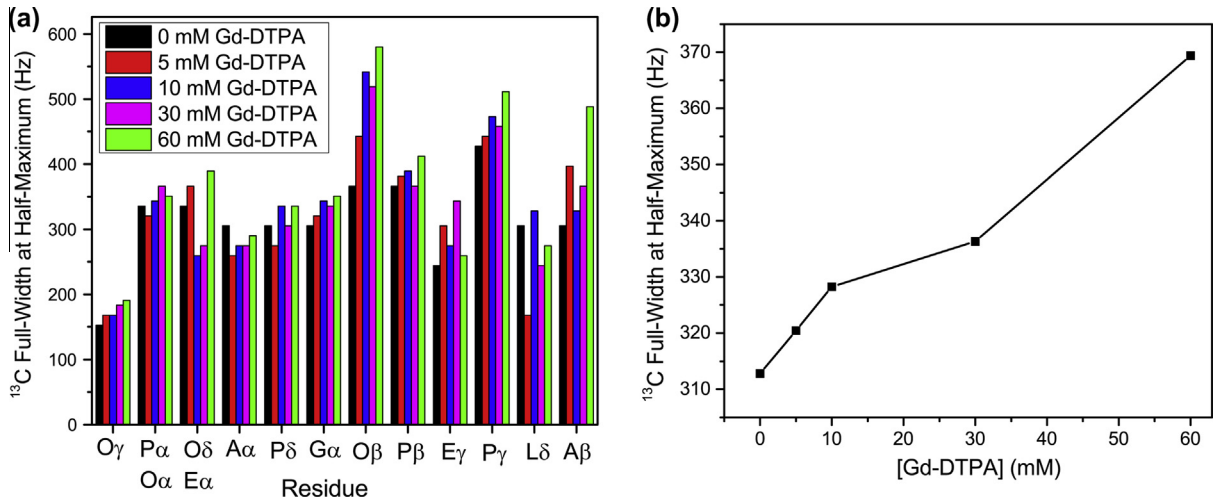

Fig. 5. (a) Carbon-13 full-width at half-maximum (FWHM) values obtained from ^{13}C ramped-CPMAS NMR spectra of bone samples under 10 kHz MAS conditions for powdered bovine cortical bone samples without Gd-DTPA (black) and with various concentrations of Gd-DTPA (red, blue, pink, green). A, alanine; L, leucine; P, proline; E, glutamic acid; O, hydroxyproline; G, glycine; CO, carbonyl. The signals from (Pα, Oα) and (Oδ, Eα) overlap in the ^{13}C NMR spectrum. (b) Gd-DTPA concentration-dependence of the average ^{13}C FWHM values calculated from (a). (For interpretation of the references to colour in this figure legend, the reader is referred to the web version of this article.)

dipolar interactions between the nuclear spins and the relaxing unpaired electrons, and they depend on the anisotropy of the magnetic susceptibility tensor for the paramagnetic ion, which describes the interaction of the paramagnetic dipole moment with the external magnetic field. Specifically, PCSs are proportional to the anisotropy of this tensor but are independent of its isotropic component [32]. In the case of Gd^{3+}, no PCSs are induced in the NMR line shapes due to the isotropic nature of its magnetic susceptibility tensor. Notably, this confirms the assertion that no undesired changes has occurred in the secondary structure and conformational dynamics of the protein and the protein–mineral surface layer in the investigated bone samples due to the addition of Gd-DTPA.

To gain a deeper insight into the site-specific paramagnetic effect of Gd-DTPA on longitudinal relaxation, the calculated ^1H T_1 relaxation times for the individual peaks (from amino acids) are shown in Fig. 4b for the doped bone samples as well as for the undoped one. In the absence of Gd-DTPA, it is observed that protons located at different positions in various amino acids exhibit different T_1 relaxation times. Most likely, these differences in the ^1H T_1 relaxation times are due to different proton–proton dipolar interactions arising from internal structural fluctuation and molecular mobility. Despite that the general trend of relaxation times as a function of the amino-acid residues is largely retained upon incubation with Gd-DTPA, the site-specific ^1H T_1 relaxation times are gradually shortened with increasing dopant concentration. For most of the amino acids, however, the ^1H T_1 values are only marginally shortened in the presence of Gd-DTPA with concentrations higher than 10 mM. Moreover, a thorough observation of the measured ^1H T_1 delays reveals that the reduction in T_1 times is not homogeneous among the ensemble of amino acid residues. Since paramagnetic relaxation enhancement by Gd^{3+} (and other ions with long electronic lifetimes) is modulated by dipolar coupling between the unpaired electronic spins and the nuclear spin, and hence is proportional to the inverse sixth power of the metal–nucleus distance [34,58], then there exists a correlation between T_1 shortening levels and residue proximity to the paramagnetic Gd^{3+} ion, which obviously implies that collagen residues located nearby the Gd^{3+} ion will exhibit more shortening in their ^1H T_1 values than the remote ones.

To examine the effect of Gd-DTPA doping on spectral resolution, the ^{13}C line widths, measured as the full width at half-maximum (FWHM) of the amino acid signals, were plotted as a function of Gd-DTPA concentration and are shown in Fig. 5. Overall, we observe that the average ^{13}C line width increases with increasing dopant concentration. However, only a marginal broadening in the line shapes is observed especially in the low-concentration range, as the average line width increases by <5% upon addition of 10 mM Gd-DTPA, and it increases by ~17% upon doping with 60 mM Gd-DTPA, which can still be considered a modest broadening. This indicates that Gd-DTPA concentrations up to 10 mM cause no pronounced effect on the ^{13}C line width, whereas higher concentrations induce only a modest broadening in the ^{13}C line shapes. These modest line broadenings can be well explained in

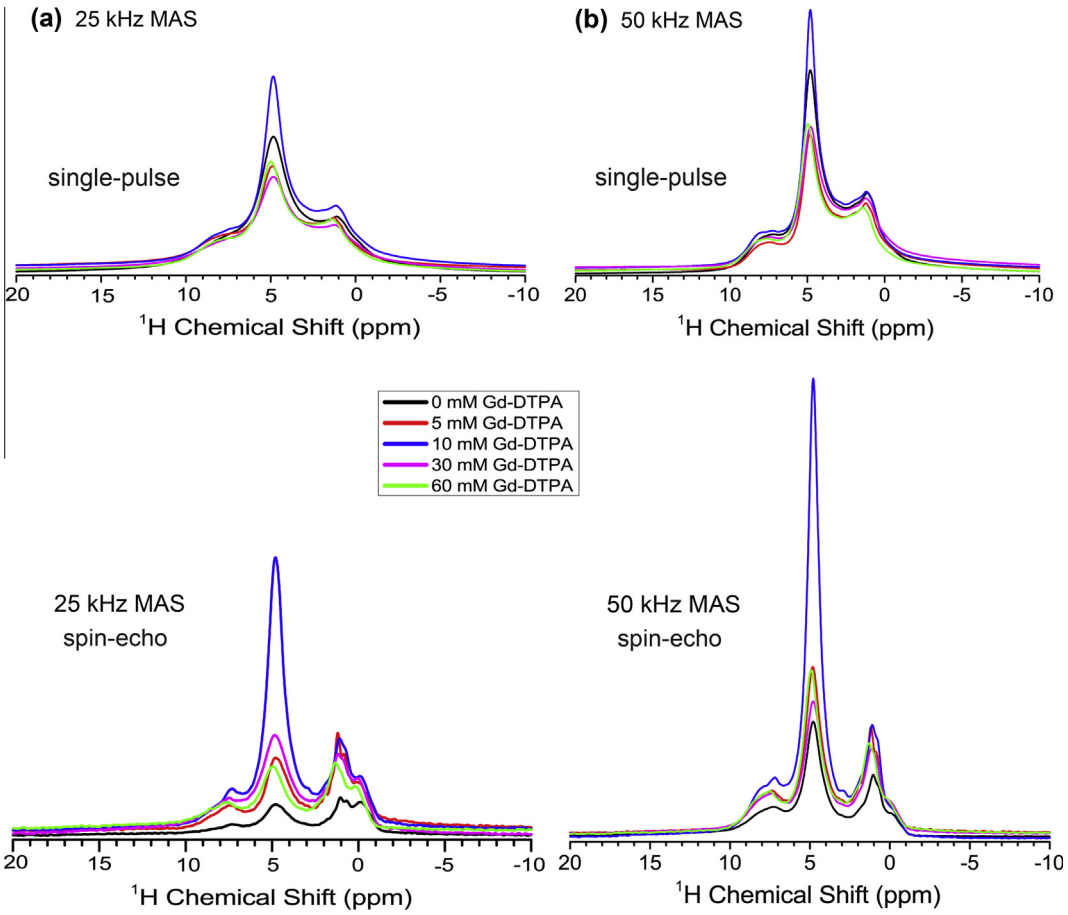

Fig. 7. ^1H MAS NMR spectra of bovine cortical bone samples at MAS rates of (a) 25 kHz and (b) 50 kHz. The experiments were acquired with either a ^1H one-pulse excitation (top row) or a rotor-synchronized spin echo (bottom row), using a 1.2 mm MAS HXY probe with a 1.2 μs $\pi/2$ ^1H-pulse. For the spin-echo experiments, an interpulse delay of 0.6 ms was used. All spectra were recorded with 64 transients, and the recycle delays were set to ~5 × ^1H T_1 for each sample as follows: 5 s for the undoped sample; 1.2 s for samples doped in 5 mM and 10 mM Gd-DTPA; and 2 s for samples doped in 30 mM and 60 mM Gd-DTPA.

terms of the transverse (T_2) PRE effects of Gd^{3+}, which is known to cause such broadenings through ^1H transverse relaxation enhancements [26]. Our experiments, however, have been designed to start with proton excitation and end with carbon detection. This implies that since the dipolar contribution of the paramagnetic transverse relaxation enhancement rates (R_2) depends on the square of gyromagnetic ratio (γ) of the observed nucleus [26,58], then the expected line broadenings caused by paramagnetic transverse relaxation are much less substantial for the ^{13}C line shapes compared to those in the ^1H line shapes (by a factor of $\sim$1/16 since $\gamma_H \approx 4\ \gamma_C$). Moreover, the ^{13}C–^{13}C spin-diffusion process is much less efficient than in the case of protons (due also to the smaller γ_C compared to γ_H), which slows down and restricts the homogeneous transfer of ^{13}C magnetization throughout the entire macromolecular lattice [48].

For the purpose of obtaining ^1H MAS NMR spectra of the bone samples at the highest possible resolution, we further investigated the effect of Gd-DTPA doping on bone NMR spectra under very fast MAS conditions. With such very high spinning frequencies, it becomes feasible to significantly reduce the line broadenings caused by the strong homonuclear ^1H–^1H dipolar couplings in the ^1H NMR line shapes. However, the issue of poor sensitivity arises in this case due to the very limited sample amounts required by the tiny rotors ($\sim$2.5–3 mg for the bone specimens used in this study). Thus, the use of Gd-DTPA doping in conjunction with very fast MAS rates is beneficial to increase the sensitivity of the NMR spectra of bones. Fig. 6 shows the ^1H T_1 time constants measured as a function of Gd-DTPA concentration at two different spinning frequencies (25 and 50 kHz) using the ^1H spin-inversion–recovery method in ^1H-detected experiments. At the magnetic field of 14.1 T, the average T_1 values are slightly shorter at 50 kHz than at 25 kHz for all of the dopant concentrations used. In accord with the ^1H T_1 data obtained from the ^{13}C-detected spectra, the 10 mM Gd-DTPA concentration is the optimum concentration that gives the maximum T_1 reduction in the ^1H-detected experiments, where a 4-fold reduction is obtained at 50 kHz MAS. Compared to the 10 mM concentration, higher Gd-DTPA concentrations produced longer ^1H T_1 relaxation times. This may be attributed to an increase in the sample temperature due to a combination of high dopant concentrations and very fast spinning speeds.

Using optimized recycle delays obtained from the measured ^1H T_1 values for each of the samples and with 25 and 50 kHz MAS rates, the 1D ^1H single-pulse and spin-echo MAS NMR spectra were acquired for the doped and undoped bone samples (Fig. 7). The ^1H single-pulse spectra of bone exhibit three main peaks, which are dominated by the intense signal from water centered at $\sim$5 ppm. In addition to this intense water signal, the other broader peaks in the ^1H single-pulse NMR spectra originate from overlapping signals that correspond to protons in the organic and mineral components of bone. It is obvious that the sensitivity is considerably improved in the spectra acquired with higher spinning speed of 50 kHz compared to those at 25 kHz. The sizeable gain in signal intensity due to Gd-DTPA doping is also obvious in the single-pulse spectra at both spinning speeds. Specifically, among the doped samples, the one doped in 10 mM GD-DTPA gives spectra with the largest increase in S/N per unit time ($\sim$2-fold increase) compared to the undoped one. Due to different transverse dephasing rates of the signals, better improvement in both resolution and sensitivity can be achieved in the spin-echo NMR spectra, which exhibit more resolved peaks compared to the single-pulse spectra. In the spin-echo spectra acquired with 50 kHz MAS rate, for example, more than $\sim$3-fold gain in overall S/N is achieved for bone doped in 10 mM Gd-DTPA. All in all, our ^1H-detected MAS NMR results demonstrate the additional benefits offered by paramagnetic doping, when combined with ultrafast spinning rates, for the sensitivity enhancement in biomolecular NMR studies of complex heterogeneous solids, particularly for samples that are only available in limited amounts.

4. Conclusions

Paramagnetic doping is arguably the simplest and most practical approach for sensitivity enhancement in multidimensional solid-state NMR spectroscopy. This robust approach has been applied here on bone samples, and the obtained results demonstrate that the widely used MRI contrasting agent Gd-DTPA is also beneficial for enhancing the proton longitudinal relaxation rates, and thereby reducing the measurement time, with minimal line broadenings and no chemical shift perturbations in ^{13}C CPMAS ssNMR of heterogeneous complex systems like bones. Doping of finely powdered bones in as low as 10 mM Gd-DTPA solution results in 3.5-fold enhancement in the intrinsic spin–lattice relaxation rates of protons in carbon-detected experiments, which is approximately 1.6 times faster compared to bone samples doped in 30 mM Cu-EDTA. Under the experimental conditions used in this study, the S/N improvement per unit time afforded by Gd-DTPA is $\sim$1.3 times better than for Cu-EDTA, while a 3-fold lower concentration is needed. This lower dopant concentration is favorable for reducing complications that may arise from sample heating and undesired dopant–bone interactions. In addition to Gd-DTPA, a number of gadolinium-based MRI contrast-enhancement agents have been successfully used in NMR for the structural elucidation of biomolecular systems [32,34,36,48]. Larger paramagnetic relaxation enhancements than with Gd-DTPA can be achieved in future studies on bone samples using other paramagnetic relaxation agents to further maximize signal enhancements of the bone organic matrix resonances. We believe that our results presented in this study would facilitate multidimensional solid-state NMR experiments for high-resolution structural and dynamic studies of various biomolecules in bone and other challenging macromolecular systems.

Acknowledgments

This research was supported by the US National Institutes of Health (NIH) grants AR056657 and AR052010, and funds from the University of Michigan to purchase the 500 MHz solid-state NMR spectrometer (to A.R.).

Appendix A. Supplementary material

Supplementary data associated with this article can be found, in the online version, at http://dx.doi.org/10.1016/j.jmr.2014.04.020.

References

[1] C. Bonhomme, C. Gervais, D. Laurencin, Recent NMR developments applied to organic–inorganic materials, Prog. Nucl. Magn. Reson. Spectrosc. 77 (2014) 1–48.
[2] M.J. Knight, I.C. Felli, R. Pierattelli, L. Emsley, G. Pintacuda, Magic angle spinning NMR of paramagnetic proteins, Acc. Chem. Res. 46 (2013) 2108–2116.
[3] M. Tang, G. Comellas, C.M. Rienstra, Advanced solid-state NMR approaches for structure determination of membrane proteins and amyloid fibrils, Acc. Chem. Res. 46 (2013) 2080–2088.
[4] A. Ramamoorthy, Beyond NMR spectra of antimicrobial peptides: dynamical images at atomic resolution and functional insights, Solid State Nucl. Magn. Reson. 35 (2009) 201–207.
[5] A. McDermott, Structure and dynamics of membrane proteins by magic angle spinning solid-state NMR, Annu. Rev. Biophys. 38 (2009) 385–403.
[6] G. Cho, Y. Wu, J.L. Ackerman, Detection of hydroxyl ions in bone mineral by solid-state NMR spectroscopy, Science 300 (2003) 1123–1127.
[7] M.J. Duer, T. Friscic, R.C. Murray, D.G. Reid, E.R. Wise, The mineral phase of calcified cartilage: its molecular structure and interface with the organic matrix, Biophys. J. 96 (2009) 3372–3378.

[8] Y.Y. Hu, A. Rawal, K. Schmidt-Rohr, Strongly bound citrate stabilizes the apatite nanocrystals in bone, Proc. Natl. Acad. Sci. USA 107 (2010) 22425–22429.
[9] D.G. Reid, M.J. Duer, R.C. Murray, E.R. Wise, The organic–mineral interface in teeth is like that in bone and dominated by polysaccharides: universal mediators of normal calcium phosphate biomineralization in vertebrates?, Chem Mater. 20 (2008) 3549–3550.
[10] E.R. Wise, S. Maltsev, M.E. Davies, M.J. Duer, C. Jaeger, N. Loveridge, R.C. Murray, D.G. Reid, The organic–mineral interface in bone is predominantly polysaccharide, Chem. Mater. 19 (2007) 5055–5057.
[11] Y. Wu, J.L. Ackerman, H.M. Kim, C. Rey, A. Barroug, M.J. Glimcher, Nuclear magnetic resonance spin–spin relaxation of the crystals of bone, dental enamel, and synthetic hydroxyapatites, J. Bone Miner. Res. 17 (2002) 472–480.
[12] P. Zhu, J. Xu, N. Sahar, M.D. Morris, D.H. Kohn, A. Ramamoorthy, Time-resolved dehydration-induced structural changes in an intact bovine cortical bone revealed by solid-state NMR spectroscopy, J. Am. Chem. Soc. 131 (2009) 17064–17065.
[13] J. Xu, P. Zhu, M.D. Morris, A. Ramamoorthy, Solid-state NMR spectroscopy provides atomic-level insights into the dehydration of cartilage, J. Phys. Chem. B 115 (2011) 9948–9954.
[14] J. Xu, P. Zhu, Z. Gan, N. Sahar, M. Tecklenburg, M.D. Morris, D.H. Kohn, A. Ramamoorthy, Natural-abundance 43Ca solid-state NMR spectroscopy of bone, J. Am. Chem. Soc. 132 (2010) 11504–11509.
[15] R.K. Rai, N. Sinha, Dehydration-induced structural changes in the collagen-hydroxyapatite interface in bone by high-resolution solid-state NMR spectroscopy, J. Phys. Chem. C 115 (2011) 14219–14227.
[16] E.E. Wilson, A. Awonusi, M.D. Morris, D.H. Kohn, M.M.J. Tecklenburg, L.W. Beck, Highly ordered interstitial water observed in bone by nuclear magnetic resonance, J. Bone Miner. Res. 20 (2005) 625–634.
[17] E.E. Wilson, A. Awonusi, M.D. Morris, D.H. Kohn, M.M. Tecklenburg, L.W. Beck, Three structural roles for water in bone observed by solid-state NMR, Biophys. J. 90 (2006) 3722–3731.
[18] M.E. Launey, M.J. Buehler, R.O. Ritchie, On the mechanistic origins of toughness in bone, Annu. Rev. Mater. Res. 40 (2010) 25–53.
[19] X. Wang, R.A. Bank, J.M. TeKoppele, C.M. Agrawal, The role of collagen in determining bone mechanical properties, J. Orthop. Res. 19 (2001) 1021–1026.
[20] S. Weiner, H.D. Wagner, The material bone: structure–mechanical function relations, Annu. Rev. Mater. Sci. 28 (1998) 271–298.
[21] H.A. Lowenstam, S. Weiner, On Biomineralization, Oxford University Press Inc., New York, 1989.
[22] A.L. Boskey, P.G. Robey, The Composition of Bone, in: Primer on the Metabolic Bone Diseases and Disorders of Mineral Metabolism, John Wiley & Sons Inc., 2013, pp. 49–58.
[23] F. Wehrli, M. Fernández-Seara, Nuclear magnetic resonance studies of bone water, Ann. Biomed. Eng. 33 (2005) 79–86.
[24] M. Renault, A. Cukkemane, M. Baldus, Solid-state NMR spectroscopy on complex biomolecules, Angew. Chem. Int. Ed. 49 (2010) 8346–8357.
[25] F.A. Perras, J. Viger-Gravel, K.M.N. Burgess, D.L. Bryce, Signal enhancement in solid-state NMR of quadrupolar nuclei, Solid State Nucl. Magn. Reson. 51–52 (2013) 1–15.
[26] S. Cai, C. Seu, Z. Kovacs, A.D. Sherry, Y. Chen, Sensitivity enhancement of multidimensional NMR experiments by paramagnetic relaxation effects, J. Am. Chem. Soc. 128 (2006) 13474–13478.
[27] N.P. Wickramasinghe, M. Kotecha, A. Samoson, J. Past, Y. Ishii, Sensitivity enhancement in (13)C solid-state NMR of protein microcrystals by use of paramagnetic metal ions for optimizing (1)H T(1) relaxation, J. Magn. Reson. 184 (2007) 350–356.
[28] D.L. Bryce, G.M. Bernard, M. Gee, M.D. Lumsden, K. Eichele, R.E. Wasylishen, Practical aspects of modern routine solid-state multinuclear magnetic resonance spectroscopy: one-dimensional experiments, Can. J. Anal. Sci. Spectrosc. 46 (2001) 46–82.
[29] T. Fujiwara, A. Ramamoorthy, How Far Can the Sensitivity of NMR Be Increased?, in: G.A. Webb (Ed.), Annual Reports on NMR Spectroscopy, Academic Press, 2006, pp. 155–175.
[30] R. Tycko, NMR at low and ultralow temperatures, Acc. Chem. Res. 46 (2013) 1923–1932.
[31] S. Ganapathy, A. Naito, C.A. McDowell, Paramagnetic doping as an aid in obtaining high-resolution carbon-13 NMR spectra of biomolecules in the solid state, J. Am. Chem. Soc. 103 (1981) 6011–6015.
[32] G. Otting, Protein NMR using paramagnetic ions, Ann. Rev. Biophys. 39 (2010) 387–405.
[33] F.-X. Theillet, A. Binolfi, S. Liokatis, S. Verzini, P. Selenko, Paramagnetic relaxation enhancement to improve sensitivity of fast NMR methods: application to intrinsically disordered proteins, J. Biomol. NMR 51 (2011) 487–495.
[34] G. Pintacuda, G. Otting, Identification of protein surfaces by NMR measurements with a paramagnetic Gd(III) chelate, J. Am. Chem. Soc. 124 (2002) 372–373.
[35] H. Yagi, K. Loscha, X.-C. Su, M. Stanton-Cook, T. Huber, G. Otting, Tunable paramagnetic relaxation enhancements by [Gd(DPA)3]3− for protein structure analysis, J. Biomol. NMR 47 (2010) 143–153.
[36] A. Eletsky, O. Moreira, H. Kovacs, K. Pervushin, A novel strategy for the assignment of side-chain resonances in completely deuterated large proteins using 13C spectroscopy, J. Biomol. NMR 26 (2003) 167–179.
[37] S. Hiller, G. Wider, T. Etezady-Esfarjani, R. Horst, K. Wuthrich, Managing the solvent water polarization to obtain improved NMR spectra of large molecular structures, J. Biomol. NMR 32 (2005) 61–70.
[38] K. Yamamoto, S. Vivekanandan, A. Ramamoorthy, Fast NMR data acquisition from bicelles containing a membrane-associated peptide at natural-abundance, J. Phys. Chem. B 115 (2011) 12448–12455.
[39] K. Yamamoto, J. Xu, K.E. Kawulka, J.C. Vederas, A. Ramamoorthy, Use of a copper-chelated lipid speeds up NMR measurements from membrane proteins, J. Am. Chem. Soc. 132 (2010) 6929–6931.
[40] N.P. Wickramasinghe, S. Parthasarathy, C.R. Jones, C. Bhardwaj, F. Long, M. Kotecha, S. Mehboob, L.W. Fung, J. Past, A. Samoson, Y. Ishii, Nanomole-scale protein solid-state NMR by breaking intrinsic 1HT1 boundaries, Nat. Meth. 6 (2009) 215–218.
[41] N.P. Wickramasinghe, M. Shaibat, Y. Ishii, Enhanced sensitivity and resolution in (1)H solid-state NMR spectroscopy of paramagnetic complexes under very fast magic angle spinning, J. Am. Chem. Soc. 127 (2005) 5796–5797.
[42] R. Linser, U. Fink, B. Reif, Probing surface accessibility of proteins using paramagnetic relaxation in solid-state NMR spectroscopy, J. Am. Chem. Soc. 131 (2009) 13703–13708.
[43] R. Linser, V. Chevelkov, A. Diehl, B. Reif, Sensitivity enhancement using paramagnetic relaxation in MAS solid-state NMR of perdeuterated proteins, J. Magn. Reson. 189 (2007) 209–216.
[44] M. Tang, D.A. Berthold, C.M. Rienstra, Solid-state NMR of a large membrane protein by paramagnetic relaxation enhancement, J. Phys. Chem. Lett. 2 (2011) 1836–1841.
[45] P.S. Nadaud, J.J. Helmus, S.L. Kall, C.P. Jaroniec, Paramagnetic ions enable tuning of nuclear relaxation rates and provide long-range structural restraints in solid-state NMR of proteins, J. Am. Chem. Soc. 131 (2009) 8108–8120.
[46] K. Yamamoto, M.A. Caporini, S. Im, L. Waskell, A. Ramamoorthy, Shortening spin–lattice relaxation using a copper-chelated lipid at low-temperatures – a magic angle spinning solid-state NMR study on a membrane-bound protein, J. Magn. Reson. 237 (2013) 175–181.
[47] D.M. Tesch, A.A. Nevzorov, Sensitivity enhancement and contrasting information provided by free radicals in oriented-sample NMR of bicelle-reconstituted membrane proteins, J. Magn. Reson. 239 (2014) 9–15.
[48] S. Ullrich, S. Hölper, C. Glaubitz, Paramagnetic doping of a 7TM membrane protein in lipid bilayers by Gd^{3+}-complexes for solid-state NMR spectroscopy, J. Biomol. NMR 58 (2014) 27–35.
[49] K.H. Mroue, N. MacKinnon, J. Xu, P. Zhu, E. McNerny, D.H. Kohn, M.D. Morris, A. Ramamoorthy, High-resolution structural insights into bone: a solid-state NMR relaxation study utilizing paramagnetic doping, J. Phys. Chem. B 116 (2012) 11656–11661.
[50] J. Schaefer, E.O. Stejskal, Carbon-13 nuclear magnetic resonance of polymers spinning at the magic angle, J. Am. Chem. Soc. 98 (1976) 1031–1032.
[51] P. Caravan, J.J. Ellison, T.J. McMurry, R.B. Lauffer, Gadolinium(III) chelates as MRI contrast agents: structure, dynamics, and applications, Chem. Rev. 99 (1999) 2293–2352.
[52] R.B. Lauffer, Paramagnetic metal complexes as water proton relaxation agents for NMR imaging: theory and design, Chem. Rev. 87 (1987) 901–927.
[53] NIST Critically Selected Stability Constants of Metal Complexes: Version 8.0, in: NIST Standard Reference Database 46, National Institute of Standards and Technology (NIST), Gaithersburg, MD, 2010.
[54] G. Metz, X.L. Wu, S.O. Smith, Ramped-amplitude cross polarization in magic-angle-spinning NMR, J. Magn. Reson., Ser. A 110 (1994) 219–227.
[55] A.E. Bennett, C.M. Rienstra, M. Auger, K.V. Lakshmi, R.G. Griffin, Heteronuclear decoupling in rotating solids, J. Chem. Phys. 103 (1995) 6951–6958.
[56] P.S. Nadaud, J.J. Helmus, I. Sengupta, C.P. Jaroniec, Rapid acquisition of multidimensional solid-state NMR spectra of proteins facilitated by covalently bound paramagnetic tags, J. Am. Chem. Soc. 132 (2010) 9561–9563.
[57] A.E. Aliev, Solid-state NMR studies of collagen-based parchments and gelatin, Biopolymers 77 (2005) 230–245.
[58] I. Solomon, Relaxation processes in a system of two spins, Phys. Rev. 99 (1955) 559–565.